

Quantitative evaluation of metal artifact reduction for coiled aneurysms in cone-beam CT

D. Ruijters¹, P. van de Haar¹, G. Kaila², T. Grünhagen¹, J. Moret³, L. Spelle³

¹Philips Healthcare, Best, the Netherlands, ²Trinity College Dublin, Ireland, ³Hôpital Bicêtre, Hôpitaux universitaires Paris-Sud, Paris, France

Hôpital Bicêtre
Hôpitaux universitaires Paris-Sud



Background and purpose

Peri-interventional Cone-beam CT (CBCT) can be used to inspect the cerebral tissue for hemorrhages and ventricular abnormalities [1]. During minimally invasive embolization of brain aneurysms the aneurysm sac is filled with metal coils [2]. The post-coiling CBCT image quality is impaired by artifacts originating from the radiopaque metal mass. The artifact streaks run through the brain parenchyma, which hampers its inspection for hemorrhages and other events. Metal artifact reduction (MAR) improves the image quality of cone-beam CT affected by streak artifacts [3].

While several metal artifact reduction schemes have been described in the literature [3,4], there is little objective quantitative evaluation on clinical data. We used pre- and post-coiling CBCT data, and applied a metric (peak signal-to-noise ratio) to quantify the improvement in image quality.

Materials and methods

For 22 retrospective aneurysm coiling cases, cone-beam CT acquisitions prior and post embolization were available. The former dataset was used as gold standard reference to evaluate the latter without and with metal artifact reduction (Figure 1). To this purpose the pre- and post-coiling datasets were co-registered [5], and the brain cavity and coiling mass were segmented [6]. The peak signal-to-noise ratio (PSNR) metric [7] was then calculated for the Hounsfield values in the brain parenchyma segment (Figure 2).

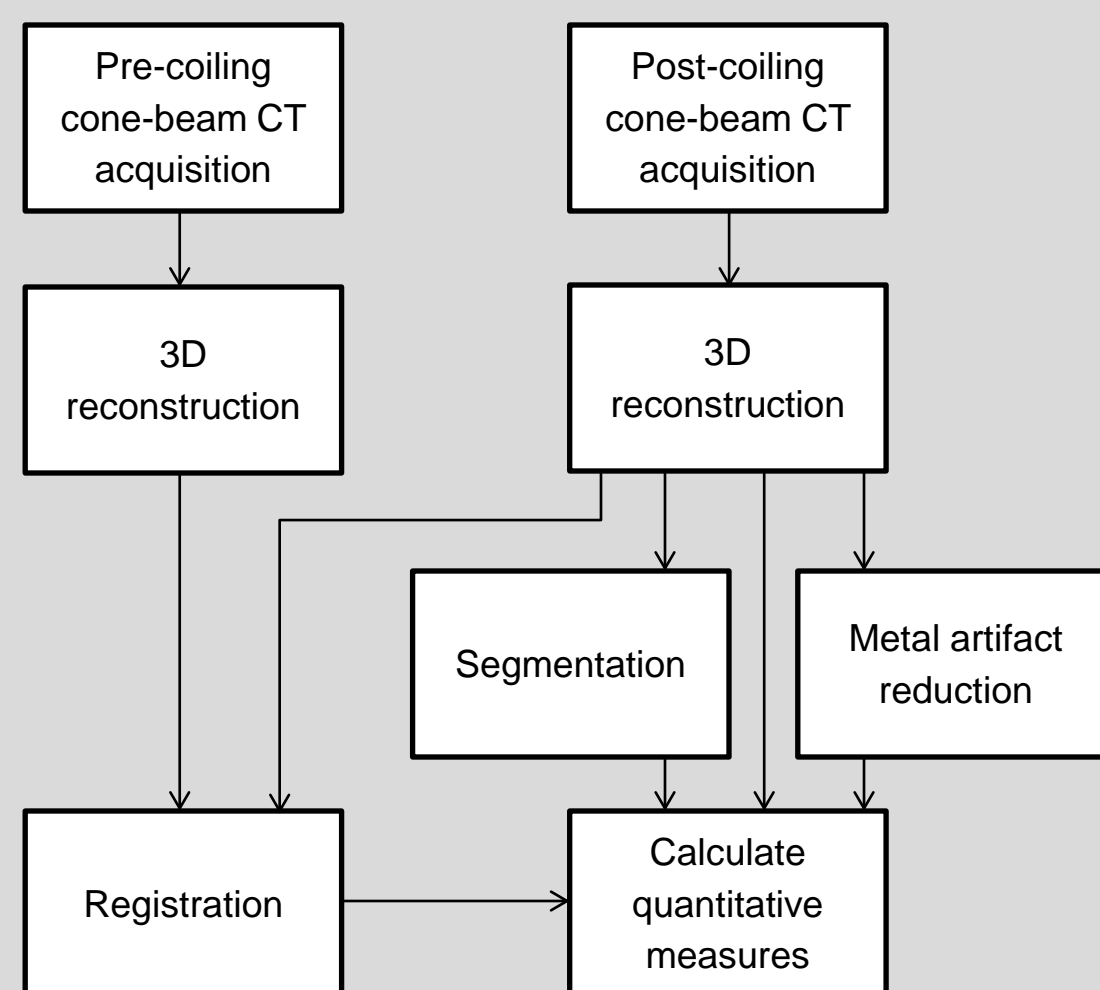


Figure 1: Data processing workflow

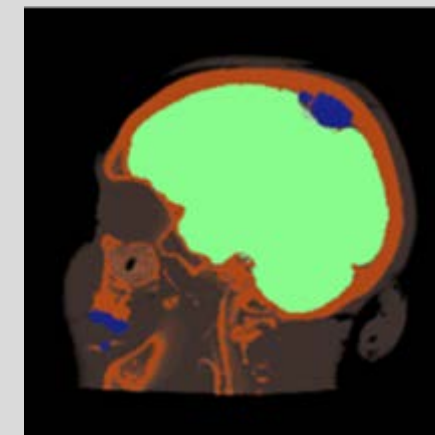


Figure 2: The cone-beam CT data is segmented into skull, metal, brain parenchyma, and other soft-tissue. The PSNR metric is only computed for the brain parenchyma segment, shown in green.

The mean squared error (MSE) is defined as:

$$MSE = \frac{1}{N} \sum_{x \in S} [T(x) - R(m(x))]^2$$

whereby S is the set of voxel positions in the segmented region, N is the number of voxels in S , T is the Hounsfield unit in the test dataset and R in the reference dataset, $m(x)$ is the co-registration mapping. The PSNR can then be calculated by:

$$PSNR = 20 \cdot \log_{10} \left(\frac{I_{max}}{\sqrt{MSE}} \right)$$

with I_{max} being the maximal Hounsfield unit in the datasets.

Results

The mean squared error improved for 20 out of 22 patients after metal artifact reduction was applied (Figure 3 & 4). The average mean squared error was reduced by 264 HU². The PSNR was improved by 6.8 dB. The average additional computation time for the metal artifact reduction algorithm amounted 20 seconds.

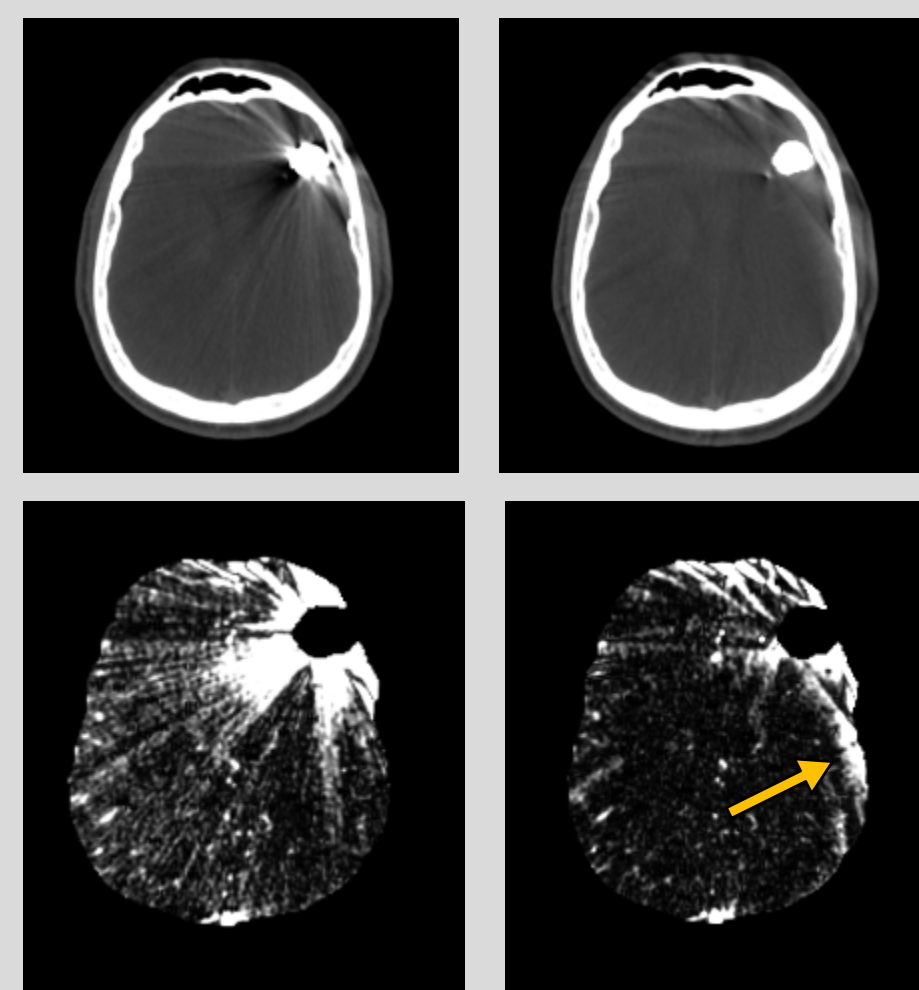


Figure 3: Left top: CBCT without metal artifact reduction (MAR). Right top: CBCT with MAR. Left bottom: subtraction of CBCT without MAR and gold standard (narrow window). Right bottom: subtraction of CBCT with MAR and gold standard. The arrow indicates artifacts that were not present originally, but have been introduced by the MAR procedure.

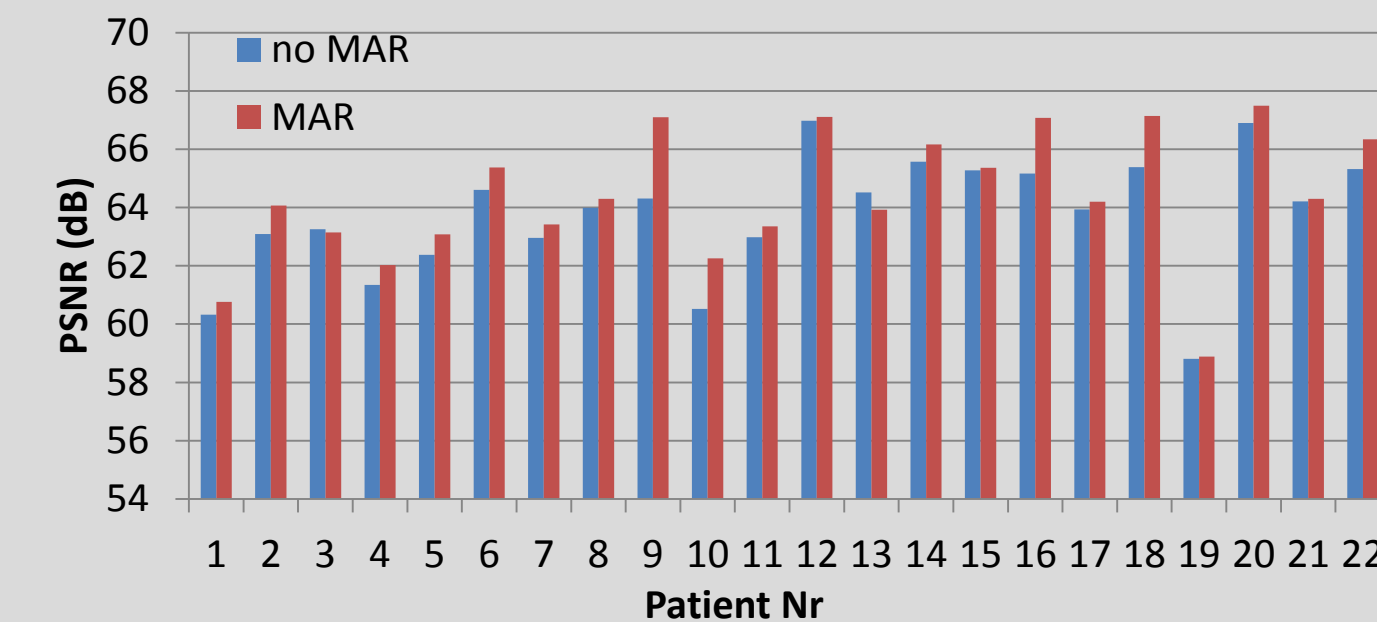


Figure 4: Peak signal-to-noise ratio (PSNR) for each patient, without metal artifact reduction (blue bars) and with metal artifact reduction (red bars).

Figure 5 shows that the mean squared error increases for larger coiled volume sizes. The regression lines for the CBCT reconstruction without and with MAR show that there is a steady improvement obtained by the MAR algorithm, slightly increasing for larger coiling volume sizes.

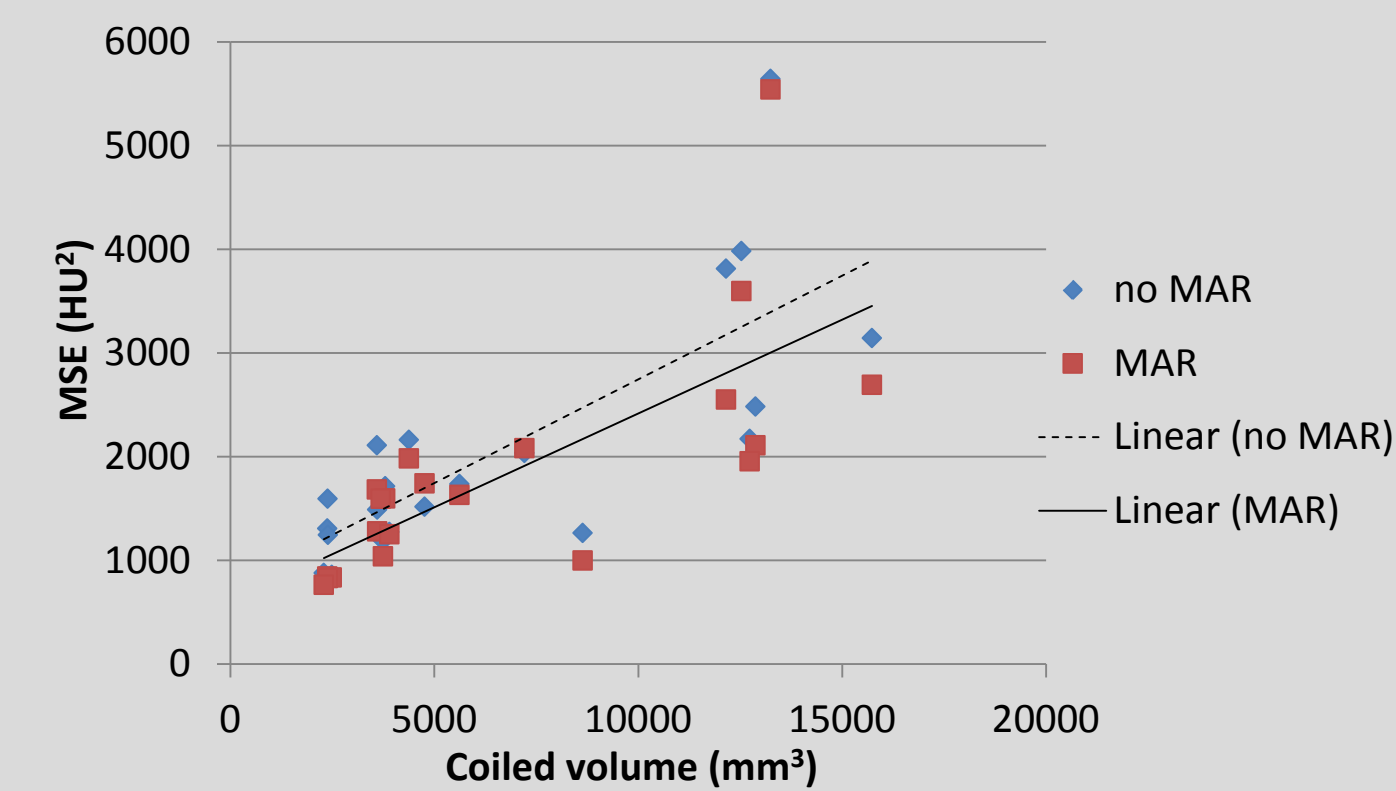


Figure 5: Correlation between coiled volume size and the mean squared error (MSE) within the brain parenchyma. Blue diamonds represent the values without MAR and red squares with MAR. The regression lines for the data points without MAR (dotted) and with MAR (solid) are also presented.

Discussion

The metal artifact reduction algorithm clearly decreases the impact of the coiling mass on the image quality, as can be seen from Figures 3 & 4. The outline of the aneurysm sac filled with metal coils is clearly visible in the MAR reconstruction, as opposed to the reconstruction without MAR. Also the deep streaks directly around the aneurysm have been considerably reduced. However, there are still remaining artifacts around the aneurysm, and while overall the artifacts have been reduced, sometimes new artifacts arise, e.g. in Figure 3 bottom row near the skull.

Prior publications have used a subjective evaluation of the image quality by clinical experts [8,9,10], or used the standard deviation of the Hounsfield values within a region of interest as a quantitative measure for the performance of the MAR algorithm [4,8,11], whereby a smaller standard deviation accounts for a more homogenous region. This latter approach, however, does not take into account that the brain parenchyma possesses natural variations of density, and it does not guarantee that the reconstructed Hounsfield levels are in fact correct. While a lower standard deviation may hint that the MAR algorithm performs properly, it is not an absolute evaluation method. In this work we have aimed to introduce an approach that does not suffer from this limitation, while being objective and quantitative. In this sense it is comparable to [8], where also a slice-wise Pearson correlation of the coiled CBCT data (with and without MAR) and pre-coiling data was performed.

Conclusion

Metal artifact reduction has been found to objectively improve the image quality quantified by the peak signal-to-noise ratio for most patients. It is therefore considered a useful tool for interventional use when the image contains metal parts.

References

- Söderman et al. Brain imaging with a flat detector c-arm. *Neuroradiology* 2008;50:863-868
- Piotin et al. Stent-assisted coiling of intracranial aneurysms: Clinical and angiographic results in 216 consecutive aneurysms. *Stroke* 2010;41:110-115
- van der Bom et al. Reduction of Coil Mass Artifacts in High-Resolution Flat Detector Conebeam CT of Cerebral Stent-Assisted Coiling. *AJNR Am J Neuroradiol* 2013;34:2163-2170
- Hung et al. Artifact reduction of different metallic implants in flat detector C-arm CT. *AJNR Am J Neuroradiol* 2014;35(7):1288-1292
- Ruijters et al. GPU-accelerated elastic 3D image registration for intra-surgical applications. *Comput Methods Programs Biomed* 2011;103(2):104-112
- Smit-Ockeloen et al. Accuracy assessment of CBCT-based volumetric brain shift field. *LNCS Clinical image-based procedures. From planning to intervention* 2016;9401:1-9
- Huynh-Thu, Ghanbari. Scope of validity of PSNR in image/video quality assessment. *Electronics Letters* 2008;44(13):800-801
- Mennecke et al. Evaluation of a metal artifact reduction algorithm applied to post-interventional flat detector CT in comparison to pre-treatment CT in patients with acute subarachnoid haemorrhage. *Eur Radiol* 2016
- Pjontek et al. Metal artifact reduction for flat panel detector intravenous CT angiography in patients with intracranial metallic implants after endovascular and surgical treatment. *J NeuroIntervent Surg* 2015;0:1-6
- Yuki et al. High-Resolution C-Arm CT and Metal Artifact Reduction Software: A Novel Imaging Modality for Analyzing Aneurysms Treated with Stent-Assisted Coil Embolization. *AJNR Am J Neuroradiol* 2016;37:317-23
- Prell et al. Metal artifact reduction for clipping and coiling in interventional C-arm CT. *AJNR Am J Neuroradiol* 2010;31(4):634-639